Atmos. Chem. Phys. Discuss., https://doi.org/10.5194/acp-2018-996
Manuscript under review for journal Atmos. Chem. Phys.
Discussion started: 30 November 2018
© Author(s) 2018. CC BY 4.0 License.

Atmospheric Chemistry and Physics Discussions

NH_3-promoted hydrolysis of NO_2 induces explosive growth in HONO

Wanyun Xu[1], Ye Kuang[2,*], Chunsheng Zhao[3], Jiangchuan Tao[2], Gang Zhao[3], Yuxuan Bian[4], Yingli Yu[3], Chuanyang Shen[3] , Linlin Liang[1], Gen Zhang[1]

[1] State Key Laboratory of Severe Weather, Key Laboratory for Atmospheric Chemistry, Institute of Atmospheric Composition, Chinese Academy of Meteorological Sciences, Beijing, 100081, China.

2 Institute for Environmental and Climate Research, Jinan University, Guangzhou, China.

[3] Department of Atmospheric and Oceanic Sciences, School of Physics, Peking University, Beijing, China

[4] State Key Laboratory of Severe Weather, Chinese Academy of Meteorological Sciences, Beijing, 100081, China

Corresponding author: Ye Kuang (kuangye@jnu.edu.cn)

Abstract

The study of atmospheric nitrous acid (HONO), which is the primary source of OH radicals, is crucial to atmospheric photochemistry and heterogeneous chemical processes. The heterogeneous NO_2 chemistry under haze conditions was pointed out to be one of the missing sources of HONO on the North China Plain, producing sulfate and nitrate in the process. However, controversy exists between various proposed mechanisms, mainly debating on whether SO_2 directly takes part in the HONO production process and what roles NH_3 and the pH value play in it. In this paper, never before seen explosive HONO production (maximum rate: 16 ppb/hour) was reported and evidence was found for the first time in field measurements during fog episodes (usually with pH>5) and haze episodes under high relative humidity (usually with pH<5), that NH_3 was the key factor that promoted the hydrolysis of NO_2, leading to explosive growth of HONO and nitrate under both high and lower pH conditions. The results also suggest that SO_2 does not directly take part in the HONO formation, but was indirectly oxidized upon the photolysis of HONO through subsequent radical mechanisms. Aerosol hygroscopicity significantly increased with the rapid inorganic secondary aerosol formation further promoting the HONO production. For future photochemical and aerosol pollution abatement, it is crucial to introduce effective NH_3 emission control measures, since the NH_3-promoted NO_2 hydrolysis is a large daytime HONO source, releasing large amounts of OH radicals upon photolysis, which will contribute largely to both atmospheric photochemistry and secondary aerosol formation.

Atmos. Chem. Phys. Discuss., https://doi.org/10.5194/acp-2018-996
Manuscript under review for journal Atmos. Chem. Phys.
Discussion started: 30 November 2018
© Author(s) 2018. CC BY 4.0 License.

1 Introduction

Nitrous acid (HONO) plays a vital role in atmospheric chemistry due to the fact that its photolysis is a major source (Michoud et al., 2014;Kleffmann et al., 2005) of hydroxyl radical (OH) which determines the atmospheric oxidative capacity and plays crucial role in tropospheric chemistry in processes such as the ozone formation, the degradation of volatile organic compounds and the secondary aerosol formation (Cheng et al., 2016;Wang et al., 2016b). Hence, the source study of nitrous acid (HONO) is of crucial importance for the understanding of the tropospheric chemistry, for chemistry and climate modelling and for developing effective pollution control strategies (Lu et al., 2018).

The North China Plain (NCP) is troubled by the persistent complex air pollution with high loadings of both photochemical pollutants and particulate pollution (Zheng et al., 2015;Ran et al., 2011) and the simultaneous mitigation of the two types of pollution has encountered trouble due to the nonlinear dependence of ozone on NOx (Xing et al., 2018). Unknown daytime sources of HONO caught attention during the past few years (Michoud et al., 2014;Liu et al., 2014;Su et al., 2011) and results from a recent study indicate that an additional missing source is required to explain more than 50% of observed HONO concentration in the daytime in Western China (Huang et al., 2017). Results from several recent studies demonstrate that intense heterogeneous conversion of NO_2 to HONO on particle surfaces might be a significant source of HONO (Liu et al., 2014;Cui et al., 2018).

Two main HONO heterogeneous production pathways involving aerosol water and NO_2 were proposed. In light of drastic decrease of solar radiation during severe haze events and rich ammonia conditions on the NCP, the first pathway hypothesized that NO_2 (g) dissolved in aerosol water at aerosol pH > 5.5 rapidly formed HONO while oxidizing HSO_3^- (aq) to sulfate. The stoichiometry of this mechanism is as follows (Cheng et al., 2016;Wang et al., 2016a):

$$2NO_2\,(aq) + HSO_3^-\,(aq) + H_2O\,(l) \Rightarrow 2H^+ + HSO_4^-\,(aq) + 2NO_2^-\,(aq). \quad (R1)$$

Based on this mechanism, good agreement between modelled and observed sulfate formation rates were achieved. However, the assumption that the pH of ambient aerosols can reach beyond 5.5 is a debatable issue. Results from several most recent studies indicate that the pH of

© Author(s) 2018. CC BY 4.0 License.

ambient aerosols fall in the range of 3-5 in most cases (Ding et al., 2018;Liu et al., 2017a;Song et al., 2018). Given this, it was proposed that HONO and NO_2^- were produced in the hydrolysis process of NO_2, releasing OH radicals upon photolysis, which indirectly oxidize SO_2 to sulfate (Li et al., 2018b):

$$2NO_2\ (g) + H_2O\ (l) \Rightarrow H^+ + NO_3^-\ (aq) + HONO. \quad (R2)$$

Results of Yabushita et al. (2009) suggest that anions greatly enhance the hydrolysis of NO_2 on water, and the NO_2 uptake coefficients of R2 can be enhanced several orders of magnitude by increasing electrolyte concentration. The ambient aerosol particles in the boundary layer are in aqueous phase under high RH (Liu et al., 2017b) and the aerosol or fog water is not pure with different dissolved anions (Wu et al., 2018;Lu et al., 2010). Therefore, HONO and nitrate formed through this mechanism should be independent of aerosol acidity, and should be primarily affected by the aerosol surface area density, aerosol liquid water content and NO_2 concentration (Li et al., 2018b). Moreover, recent theoretical simulations have proposed a HONO formation mechanism involving NO_2 and water and have identified that NH_3 can promote the hydrolysis of NO_2 (Li et al., 2018a) (R2). Despite of this, no direct evidence from field observations were available in this paper to support their findings.

Although the proposed HONO formation mechanisms are all heterogeneous reactions of NO_2, the details of how SO_2, pH and NH_3 are involved in heterogeneous formation are still under debate (Li et al., 2018b) and a clear mechanism is still missing in current models to explain both the daytime concentration of observed HONO and the secondary inorganic aerosol formation. Measurements of HONO are rare and simultaneous observations of HONO and aerosol physical and chemical characteristics are lacking to thoroughly analyze or directly support the aerosol heterogeneous HONO formation mechanisms involving NO_2. In this paper, we present for the first time simultaneous measurements of HONO, sulfate and nitrate as well as other precursor gases, oxidants and meteorological parameters during both fog and haze episodes under high ambient RH. Fog water pH is usually greater than 5.5 in eastern China (Safai et al., 2008;Lu et al., 2010), while calculations in this work and previous studies collectively indicate a moderately acidic condition ($4<pH<5$) for fine particles in northern China winter haze. The observational results unveil that NH_3 is the key factor that promotes the hydrolysis of NO_2, resulting in explosive formation of HONO, nitrate and sulfate.

Atmos. Chem. Phys. Discuss., https://doi.org/10.5194/acp-2018-996
Manuscript under review for journal Atmos. Chem. Phys.
Discussion started: 30 November 2018
© Author(s) 2018. CC BY 4.0 License.

Atmospheric Chemistry and Physics Discussions

2 Site description and instruments

From 15th Oct. to 25th Nov. 2016, a field campaign intended to study sulfate formation was conducted at the Ecological and Agricultural Meteorology Station ($39°09'N, 115°44'$E) of the Chinese Academy of Meteorological Sciences. The site is partly composed of experimental farmland and is also surrounded by farmland and small residential towns (nearest town ~1.5 km). It is located between Beijing (~ 100km) and Baoding (~40km), two megacities on the North China Plain (Fig. 1). During this field campaign, an In situ Gas and Aerosol Compositions Monitor (IGAC, Fortelice International Co.,Taiwan) was used for monitoring water-soluble ions (Na^+, K^+, Ca^{2+}, Mg^{2+}, NH_4^+, SO_4^{2-}, NO_3^-,NO_2^-, Cl^-) of $PM_{2.5}$ (particulate matter with aerodynamic diameter less than 2.5 μm) and trace gases including HONO, SO_2, NH_3, HCl, and HNO_3 with a time resolution of 1h. The IGAC system draws in ambient air through a PM10 inlet and passes the sample through a sharp-cut PM2.5 cyclone at a flowrate of 16.7 L/min. A vertical annular denuder wetted with dilute H_2O_2 solution collects the trace gases. A scrub and impact aerosol collector under the denuder is mounted at an inclined angle to capture particles based on impaction after condensation growth. Two separate Ion Chromatographs are used to respectively analyze anions and cations for the gas and aerosol liquid extracts which were injected from the denuder and the aerosol collector once an hour. The detection limits are below 0.12 μg/m^3 and the background concentration of most water-soluble inorganic ions within the instrument were below 0.11 μg/m^3, only with SO_4^{2-} showing a background concentration of 1.10 μg/m^3 (Young et al., 2016). Under highly polluted conditions such as our site, these measurement uncertainties are fully acceptable. The instrument has shown good performance in the past, agreeing well with filter based samples (Liu et al., 2017a). Standard LiBr solution was continuously added to the aerosol liquid extracts during the measurements, to ensure the sampling and analyzing process is stable. The swing amplitude was within the range of three standard deviation, confirming the stability of the ion analyzing system throughout the campaign. A mixed standard solution was diluted to perform multipoint calibrations (at 5, 10, 20, 50, 100, 200, 500 and 1000 ppb concentrations) at the beginning and at the end of the campaign for the ions Na^+, K^+, Ca^{2+}, Mg^{2+}, NH_4^+, Li^+, SO_4^{2-}, NO_3^-,NO_2^-, Cl^-, Br^-, with the R^2 of the calibrations reaching above 0.9999.

NOx and CO were observed using commercial instruments from Thermo Electronics (Model 42CTL and 48CTL), while the Aerolaser AL2021 H_2O_2-monitor was used to measure H_2O_2 concentrations. The ambient RH, temperature, wind speed and wind direction were observed

© Author(s) 2018. CC BY 4.0 License.

using an automatic weather station. The dry state particle number size distributions (PNSDs) in the diameter range of 3nm to 10μm, were jointly measured by a scanning mobility particle size spectrometer (SMPS) and an Aerodynamic Particle Sizer (APS, TSI Inc., Model 3321). The ambient aerosol liquid water concentrations were calculated based on measurements of a three-wavlength humidified nephelometer system (Kuang et al., 2018). The aerosol hygroscopicity parameter κ (Petters and Kreidenweis, 2007) is calculated using the method proposed by Kuang et al. (2017).

3 Observed simultaneous rapid increase of HONO, nitrate and sulfate

The time series of HONO, sulfate, nitrate and ammonium and precursor gases, meteorological parameters and other parameters are shown in Fig. 2. During this observation period, HONO concentration ranged from 0.31 to 17.6 ppb (ranged from 0.3 to 6.0 ppb during most periods) with an average of 3.0 ppb. The HONO/NO_2 ratio ranged from 0.03 to 0.75 with an average of 0.18, which is higher than the average HONO/NO_2 ratio previously observed in China (Liu et al., 2014;Cui et al., 2018). NO_2 concentration ranged from 7.5 to 60.1 ppb with an average of 32.0 ppb. NH_3 concentration ranged from 0.05 to 30 ppb with an average of 12.3 ppb. Four rapid HONO formation events were identified in Fig.2, two under foggy conditions and the other two under high RH conditions.

3.1 Explosive growth of HONO during fog episodes

Two dense fog episodes with rapid HONO increase were observed for the first time in China, occurring on the 4th and 5th Nov. 2016. From satellite images (Fig. 1) it can be seen that on the 5th Nov., a wide area of the NCP was shrouded by fog before noon (about 11:30) including the observation site, however, the fog area reduced in the afternoon (about 13:30) and dissipated near the observation site. The evolution of the fog-shrouded area during these two days was also observed by a geostationary satellite (http://www.eorc.jaxa.jp/ptree/index.html). These two fog episodes offer us a great opportunity to study the hydrolysis process of NO_2 (R2) and the role of SO_2 in heterogeneous HONO production in fog water (R1), which usually show pH above 5.5 (Safai et al., 2008;Lu et al., 2010).

The time series of simultaneously observed meteorological parameters, concentrations of nitrate, ammonium, sulfate and their precursor gases SO_2, NO_2, NO and NH_3, as well as

© Author(s) 2018. CC BY 4.0 License.

atmospheric oxidants such as O_3, H_2O_2 and other parameters including CO, which is indicative of transport processes during the two days with fog episodes are shown in Fig. 3. From 0:00 (Beijing local time) on the 4th Nov., the ambient RH continuously increased and reached 100% near 5:00, and lasted about 8.5 hours before it dropped below 100% near 13:30. However, at 15:30, the ambient RH began to rise again and reached 100% near 19:30, and then sustained until 12:00 on the 5th Nov. The latter fog episode lasted about 18.5 hours.

During the first fog episode, the rapid increases of HONO, nitrate, sulfate and ammonium were observed from 8:50 to 11:30 (Case1). HONO increased from 3.6 ppb to 10.6 ppb, with the most rapid increase occurring around 11:00 at a rate of 5.5 ppb/h. During the HONO increasing period, the variation characteristics of related trace gases and other parameters are as follows. NH_3 concentration increased slowly at first and then increased drastically near 11 am (10 ppb/h). SO_2 concentration remained almost constant at first and then increased from near 0.25 ppb to 0.4 ppb. NO_2 concentration increased continuously with a small magnitude, while NO concentration increased first and then decreased. H_2O_2 concentration is continuously increasing, but O_3 concentration remained near zero. CO concentration remained almost constant (~2.5 ppm), suggesting that there was no evident plume transport during this process. Wind speed was less than 2 m/s, and dropped almost to 0 m/s when HONO concentration dramatically increased, further supporting the fact that the drastic increase was not caused by transport processes. Ammonium, nitrate and sulfate concentration steadily increased from 10.7, 5.2, 3.5 ppb to 20.5, 12.0, 7.9 ppb, respectively. A noticeable increase in nitrite was also observed, when HONO increased most rapidly. It should be noted that the cutting diameter of the IGAC instrument is 2.5 μm, which means that observed concentrations only represent the variation of inorganics ions in aerosol water, and that of fog droplets were not included.

During the second fog episode, HONO, nitrate, sulfate and ammonium started to increase rapidly from 9:30 and reached a plateau near 12:30, when the fog started to dissipate (Case2). HONO increased from 3 ppb to 9.5 ppb, with the fastest increase occurring near 11:00 at a rate of 3.5 ppb/h. Variation characteristics of other parameters are as follows. NH_3 concentration increased steadily from 5 ppb to 24 ppb. SO_2 concentration increased steadily from 0.25 ppb to 1.25 ppb. NO_2 concentration remained almost constant at the very beginning (near 40 ppb) and then increase slightly, while NO concentration remained almost constant (near 30 ppb) throughout the entire fog period. H_2O_2 concentration increased slightly at first and then rose rapidly towards

© Author(s) 2018. CC BY 4.0 License.

the end of the fog period. O_3 concentration increased very slightly. CO concentration remained also near constant (~3 ppm). Wind speed was steady and less than 2 m/s at the beginning, however, began to increase quickly at noon. Ammonium, nitrate and sulfate concentration steadily grew from 11.7, 6.7, 3.8 ppb to 22, 15.5, 8 ppb, respectively. The variation of nitrite was very similar to that of HONO. The variation of wind speed demonstrate that at the very beginning of the HONO increase, the air mass was relatively stagnant, but became windy when the fog dissipated.

3.2 Explosive growth of HONO during haze episodes with high RH conditions

The two periods with rapid HONO increase under high RH conditions occurred on the 11th and 14th Nov., respectively. The time series of simultaneously observed meteorological parameters, concentrations of nitrate, ammonium, sulfate and their precursor gases SO_2, NO_2, NO and NH_3, as well as oxidants including O_3, H_2O_2 and other parameters such as CO concentration, aerosol volume concentration in dry state and aerosol liquid water content during the two days are shown in Fig.4.

On the 11th Nov., HONO started rising from 6:30 (3.4 ppb) and came to a halt at 9:00 (11.5 ppb) (Case 3). The quickest increase of HONO occurred near 9 o'clock with a rate of 5.6 ppb/h. The key features of other parameters are introduced in the following. The ambient RH decreased rapidly (from foggy condition to near 75%). NH_3 increased slowly at first and then grew rapidly. NO_2 increased slowly and SO_2 remained low. The total volume concentration of $PM_{2.5}$ was decreasing. Ammonium, nitrate and sulfate concentrations increased very slowly at first and then evident increase was observed in ammonium and nitrate. The decrease in dry state volume concentration of $PM_{2.5}$ demonstrate that the air mass is not quite steady due to transport or boundary layer processes. The slight increase of nitrate and sulfate despite the drop in total $PM_{2.5}$ concentration suggest that the nitrate and sulfate produced during the increasing process of HONO outgrew those lost to boundary layer mixing and transport.

On the 14th Nov., HONO increased drastically near 11:00, reaching 17.6 ppb at 11:30 (16.1 ppb/h) and then dropped promptly to 4 ppb at 12:30 (Case 4). This phenomenon took place when the fog dissipated and the ambient RH abruptly dropped to near 85%. Key variation features of other parameters are as follows. NH_3 increased rapidly from 9.7 ppb to 30 ppb. NO_2 concentration was increasing quickly, while SO_2 concentration remained low. The concentration of sulfate and nitrate also increased quickly. Volume concentration of $PM_{2.5}$ was decreasing, indicating that even

© Author(s) 2018. CC BY 4.0 License.

more sulfate and nitrate were formed than the observed growth in their concentrations. The O_3 concentration stayed near zero, which means that UV radiation was weak. After the quick formation of HONO, O_3 concentration began to rise, indicating the increase in UV radiation intensity. The photolysis of HONO was high probably the cause for its drastic decrease. Note that the HONO was not increasing during the period where only NO_2 increased rapidly and NH_3 varied little.

4 Discussions

4.1 Discussions on the HONO formation mechanism

In these four rapid HONO increasing episodes, the maximum HONO growth rates (dHONO/dt) all exceed 5 ppb/h, and even reach beyond 16 ppb/h. Such high HONO growth rates as observed in this study were not yet reported in literature.

The homogeneous reaction of NO with OH is an important source of HONO and can be estimated using the equation:

$$P_{NO+OH}^{net} = k_{NO+OH}[NO][OH] - k_{HONO+OH}[HONO][OH], \quad \text{(Eq. 1)}$$

where k_{NO+OH} (7.2 × 10−12 cm^{-3} s^{-1}) and $k_{HONO+OH}$ (5.0 × 10−12 cm^{-3} s^{-1}) are the rate constants of the reactions of NO and HONO with OH, at 298 k, respectively (Li et al., 2012). Using an OH concentration of 1×10^6 cm^{-3}, typical for noontime haze conditions, the estimated homogeneous production rate are 2.04, 0.79, -0.33 and -0.37 ppb/h for the episodes on 4th, 5th, 11th and 14th Nov., respectively, showing little variability or decreases during the increase of HONO. Clearly, homogeneous oxidation of NO cannot explain the observed HONO variations.

The NO/NOx ratio during the HONO increasing episodes ranged from 0.37 to 0.76, suggesting that the air masses were relatively aged compared to freshly emitted air mass from exhaust (NO/NOx>0.9). Even if we assume all the measured NOx came from vehicle emissions and an emission ratio of 10%, which is higher than the upper limit of 8% used in Huang et al. (2017) (Huang et al., 2017), the contribution of vehicle emissions to HONO would be in the range of 0.97 to 1.09, 0.63 to 0.83, 0.73 to 1.16 and 0.9 to 1.15 ppb during the episodes on 4th, 5th, 11th and 14th Nov., respectively. Even if the emission ratio were underestimated, NOx decreased during these events with the increase in HONO, which proves that the observed HONO variation could not have been caused by direct vehicle emissions.

© Author(s) 2018. CC BY 4.0 License.

Recent studies also suggest biomass burning to be an important HONO source, mainly by increasing particle surface area and NO2 conversion efficiency (Nie et al., 2015). Under foggy conditions, surface area is not the limiting factor to the NO2 conversion. During the haze events, particle surface area was decreasing due to decreasing humidity and aerosol water content. Hence, the variation of surface area cannot explain the observed HONO increases. According to the mapped fire spots on the days of the HONO events (Fig. S2), there was no fire within 20 km distance to the site. K+ is often used as an indicator for biomass burning. The average K+ concentration during the whole campaign ranged from 0.022 to 5.95 μg/m3, with an average of 1.28 μg/m3. The K+ level during the four events were 1.39, 1.08, 1.51 and 1.54 μg/m3, respectively, showing no evident sign of biomass burning.

The fact that HONO drastically increased while NO_2 varied little (9:30 to 11:30, 5th Nov. and 6:30 to 8:30, 11th Nov.) or hardly increased even under drastic increases of NO_2 (8:30 to 11:30, 14th Nov.), but displayed explosive growth with increasing NH_3, cannot be explained by current known HONO sources (direct emission or gas phase reactions). These rapid increasing HONO phenomena were observed under foggy or under high RH conditions, which leads us to suspect that the HONO increase was caused by heterogeneous conversion of NO_2. Was it R1, R2 or another mechanism that led to the explosive growth of HONO?

Based on results from Wang et al. (2016a) and Cheng et al. (2016), R1 is more likely to happen during fog episodes or under NH_3 neutralized conditions (3,4). While R1 might be able to explain the formation of sulfate and HONO, it cannot explain that of nitrate. The observed molar increase of nitrate were always larger than that of sulfate, usually exceeding twice the amount of sulfate. In addition, pH values during the rapid HONO increasing period under high RH conditions (estimated from ISORROPIA with the forward mode and metastable assumption (Song et al., 2018), Fig. 4) were continuously below 5, further demonstrating that R1 is unlikely to happen under such conditions.

Laboratory experiments demonstrated that anions greatly enhance NO_2 uptake on water (Yabushita et al., 2009;Li et al., 2018b), which suggests that R2 is more likely to occur in fog water that is rich in anions. The concentration of NO_2 as well as the surface area density of fog droplets should be the controlling factors of the NO_2 uptake, as opposed to the pH of the water droplets. Based on the reactive uptake coefficient of NO_2 (γ_{NO_2}) in Yabushita et al. (2009), we have calculated the HONO production rate of R2 under different conditions (see Fig.S1). During foggy

© Author(s) 2018. CC BY 4.0 License.

conditions, the HONO production rate should be higher than 1 ppb/(ppb NO_2·h). The NO_2 concentration during the two fog episodes ranged between 40 to 50 ppb, therefore, the HONO production rate should be higher than 40 ppb/h during the observed fog periods according to the results in Fig.S1. However, no rapid increase of HONO was observed unless NH_3 was simultaneously increasing. This result indicates that R2 is missing the important impact of NH_3 in the heterogeneous HONO production and that the currently used γ_{NO_2} range is at least overestimated when NH_3 is not abundant enough.

Recent theoretical simulation results (Li et al., 2018a) ascertain that NH_3 can promote the hydrolysis of NO_2 and contribute to HONO formation via R2. This conclusion is consistent with the observed phenomena that HONO only increased rapidly when NH_3 was simultaneously increasing. Considering the influence of NH_3 and sulfate on the aerosol pH, under our observed NH_3 concentration range, NH_3 has negligible impact on pH values (Guo et al., 2017), especially under high RH conditions. This further proves that the NH_3-promoted hydrolysis of NO_2 is independent of the pH value.

So what role does SO_2 play in the HONO formation and what caused the rapid formation of sulfate? Li et al. (2018b) pointed out that NO_2 can oxidize S(IV) indirectly via free radical mechanism (the involved reactions RS1 to RS5 proposed in Li et al. (2018b) are listed in the supplement). The key step of the proposed S(IV) oxidation pathway is the photolysis of HONO to produce OH (RS1). Produced OH can oxidize S(IV) to form bisulfate or sulfate through reaction RS2 and produce HO_2. HO_2 can react with NO to produce NO_2, or react with itself to produce H_2O_2. Is the radiation during fog and haze events strong enough to photo dissociate the produced HONO and release large amounts of OH radicals? Diurnal evolutions of the lifetime of HONO (only considering the photolysis process) under different aerosol optical depth (AOD) and different cloud optical depth conditions are presented in Fig.5, which were calculated using the j-values simulated by the TUV radiative transfer model (version 5.3, http://www2.acom.ucar.edu/modeling/tuv, the required single scattering albedo and aerosol angstrom exponent were estimated using simultaneously measured PNSD and BC measurements (Kuang et al., 2015). The results in Fig.5a demonstrate that for AOD (550nm)=1.0, the lifetime of HONO quickly drops below 1 hour after sunrise and is less than 0.5 hour at noontime. The AOD at 550 nm observed near 13:30 by the MODIS (Moderate resolution Imaging Spectroradiometer) Aqua satellite on the 14th November is 0.7, thus, the drastic decrease of HONO on the 14th

© Author(s) 2018. CC BY 4.0 License.

November can be well explained by its rapid photolysis and the amount of OH radicals released must be even greater than the drop in HONO concentrations, since HONO was simultaneously produced via NO_2 hydrolysis. During Case 1 and 3, HONO began to decrease when NH_3 was still increasing. The reason might be that the UV radiation at that point was already strong enough to photolyze HONO quickly, which lead to the drastic drop in HONO concentrations (The diurnal evolution of lifetime of HONO under different cloud optical depth conditions are depicted in Fig.5b). O_3 started to increase quickly as HONO began to decrease, which is an indirect evidence of the increasing UV radiation. The increase in H_2O_2 during the increase of HONO in the two fog episodes, where O_3 concentration stayed near zero, might be an indirect evidence of the HO_2 production and occurrence of RS2. The formed H_2O_2 can also oxidize S(IV) to form sulfate via heterogeneous processes, even more efficient than the OH radical oxidation in the gas phase under high RH conditions. In this way, the simultaneous formation of HONO, sulfate and nitrate can be well explained and it becomes clear that SO_2 does not participate in the heterogeneous HONO production process.

Another phenomenon worth noting is that, in Case 3, HONO was increasing rapidly even under the drastic decrease in ambient RH, which demonstrates that the impact of NH_3 on HONO formation should be even more important than that of aerosol liquid water content. However, the hydrolysis of NO_2 needs water to be involved, thus, the importance of water content under different conditions remains to be elucidated.

To further investigate the acceleration effect of NH_3 on the hydrolysis of NO_2, we have examined the correlations between the NO_2-to-HONO (HONO/NO_2 ratio), NO_2-to-NO_3^- (NO_3^- /NO_2 ratio) conversion efficiencies and the NH_3 concentration during the entire field campaign (Fig.6). Note that only data points during nighttime (18 pm to 6 am) and with ambient RH Higher than 80% are shown in Fig.6. Daytime data were excluded, because HONO would quickly photolyze as soon as sunlight is available, even if there was rapid HONO production, the corresponding increase of HONO might not be observed due to its quick photolysis. The reason for only including data with ambient RH higher than 80% is because the quick hydrolysis of NO_2 requires water to be involved. However, the overall hygroscopicity of ambient aerosols during this field campaign is relatively low (average hygroscopicity parameter κ is 0.14 (Kuang et al., 2018) and the volume contribution of liquid water to the total volume concentrations of ambient aerosols is quite low when ambient RH is below 80% during this field campaign. Details on the volume

© Author(s) 2018. CC BY 4.0 License.

335 contribution of liquid water to the total volume of ambient aerosols can be referred to Kuang et al.
336 (2018). The correlation coefficient between HONO/NO_2 ratio and the NH_3 concentration reaches
337 0.68, while that between NO_3^-/NO_2 ratio and NH_3 concentration only reaches 0.48, since the source
338 of NO_3^- is much more complicated than that of HONO. These results have further verified that
339 NH_3 promotes the NO_2 hydrolysis and HONO production. The correlation of HONO/NO_2 to NH_3
340 is highly nonlinear, HONO/NO_2 increases rapidly with NH_3 when NH_3 reaches above 10 ppb.

341 **4.2 Diurnal variations of inorganic secondary aerosol formation and aerosol hygroscopicity**
342 **determined by NH_3**

343 According to the discussions in Sect.4.1, NH_3 promotes the hydrolysis of NO_2, producing
344 HONO and nitrate. During daytime, HONO photolysis further produces OH and results in
345 significant formation of sulfate. Hence, diurnal variations of NH_3 should have exerted significant
346 influences on the diurnal variations of HONO and inorganic aerosol chemical components. The
347 average diurnal variations of NO_2, NH_3, HONO as well as SO_2 concentrations during this field
348 campaign are shown in Fig.7a. The average HONO concentration during nighttime is higher than
349 that during daytime due to the quick photolysis of HONO upon solar irradiation. The NH_3
350 concentration begins to increase in the morning (near 8 o'clock) the reaches the plateau in the
351 afternoon (8.5 to 15.5 ppb in average), and the SO_2 concentrations shows a similar diurnal variation
352 to that of NH_3. This type of diurnal variation of SO_2 was also found by Xu et al. (2014), however,
353 the cause of this diurnal pattern of NH_3 and SO_2 during this field campaign requires further
354 investigation. The NO_2 concentration increases quickly in the afternoon and decreases in the
355 evening.

356 As shown in Fig.7b, the increase of NH_3 from morning to the afternoon was accompanied
357 with the increase of mass fractions of nitrate and sulfate in $PM_{2.5}$ (The mass fractions of different
358 aerosol chemical compositions were obtained by using the measured dry state PNSD to calculate
359 volume concentration of $PM_{2.5}$, assuming that the density of aerosols in dry state is 1.5 g/cm^3 (Yin
360 et al., 2015). The results shown in Fig.7b indicate that the molecular concentration increase in
361 nitrate in the morning and afternoon is much faster than that of sulfate, since the molar mass of
362 sulfate is much higher than that of nitrate, again supporting the theory of NH_3-promoted NO_2
363 hydrolysis, which only produces HONO and nitrate directly. It is noteworthy that, in the morning,
364 the evident increase of the contribution of inorganic aerosol components (sulfate, nitrate,
365 ammonium) to ambient aerosol mass resulted in prominent increases of aerosol hygroscopicity

© Author(s) 2018. CC BY 4.0 License.

(average hygroscopicity parameter κ during this field campaign is 0.14 (Kuang et al., 2017) as shown in Fig.7c. From the morning to the afternoon, the ambient RH decreases quickly, however, the increase of aerosol hygroscopicity will retard the decrease of aerosol liquid water content and surface area density of ambient aerosols. This further enhances the hydrolysis of NO_2 as well as the nitrate and sulfate formation as opposed to conditions with constant aerosol hygroscopicity.

5. Summary and atmospheric implications

Explosive HONO growth (observed maximum dHONO/dt=16.1 ppb/h) was observed for the first time on the NCP during fog and haze episodes with high RH conditions, only occurring with evident increases in NH_3, indicating that NH_3 is the key factor promoting the hydrolysis of NO_2, resulting in rapid HONO and nitrate formation. NH_3 concentration during the observation period exhibit a distinct diurnal variation with an increase in the morning and a peak in the afternoon (8.5 to 15.5 ppb in average). The increase of NH_3 promotes the hydrolysis of NO_2, giving significant rise to HONO and nitrate concentrations. Produced HONO released OH radicals upon photolysis, which further oxidized SO_2 to sulfate through gas phase and heterogeneous reactions. Therefore, the significant diurnal variations of NH_3 has determined the diurnal variations of nitrate, sulfate and ammonium as well as that of aerosol hygroscopicity.

Results in this paper reveals that the NH_3-promoted NO_2 hydrolysis is a significant source of HONO, which provides direct insight into the missing daytime source of HONO on the NCP. Results in this paper also shed light on the recent controversy of how SO_2, pH and NH_3 are involved in heterogeneous HONO production. It was clarified that SO_2 does not directly take part in the HONO production, but is a byproduct of the HONO photolysis, confirming again the importance HONO as an OH source and its crucial role in atmospheric chemistry.

These results have demonstrated the critical role and contribution of NH_3 in the formation of photochemical and aerosol pollution on the North China Plain. Effective control measures are urgently called for to reduce NH_3 emissions, which would simultaneously benefit the photochemical and aerosol pollution abatement through the reduction of HONO production.

Acknowledgments, Samples, and Data

This work is supported by the National Key R&D Program of China (2016YFC0202300), the National research program for key issues in air pollution control (DQGG0103) and the National Natural Science Foundation of China (41505107 and 41590872). We thank Wei Peng from Beijing Met High-Tech Co., Ltd. for his help with the maintenance of the IGAC instrument.

© Author(s) 2018. CC BY 4.0 License.

Data availability. The data used in this study are available from the corresponding author upon request (kuangye@jnu.edu.cn)

References

Cheng, Y., Zheng, G., Wei, C., Mu, Q., Zheng, B., Wang, Z., Gao, M., Zhang, Q., He, K., Carmichael, G., Pöschl, U., and Su, H.: Reactive nitrogen chemistry in aerosol water as a source of sulfate during haze events in China, Science Advances, 2, 10.1126/sciadv.1601530, 2016.

Cui, L., Li, R., Zhang, Y., Meng, Y., Fu, H., and Chen, J.: An observational study of nitrous acid (HONO) in Shanghai, China: The aerosol impact on HONO formation during the haze episodes, The Science of the total environment, 630, 1057-1070, 10.1016/j.scitotenv.2018.02.063, 2018.

Ding, J., Zhao, P., Su, J., Dong, Q., and Du, X.: Aerosol pH and its influencing factors in Beijing, Atmos. Chem. Phys. Discuss., 2018, 1-34, 10.5194/acp-2018-270, 2018.

Guo, H., Weber, R. J., and Nenes, A.: High levels of ammonia do not raise fine particle pH sufficiently to yield nitrogen oxide-dominated sulfate production, Scientific reports, 7, 12109, 10.1038/s41598-017-11704-0, 2017.

Huang, R.-J., Yang, L., Cao, J., Wang, Q., Tie, X., Ho, K.-F., Shen, Z., Zhang, R., Li, G., Zhu, C., Zhang, N., Dai, W., Zhou, J., Liu, S., Chen, Y., Chen, J., and O'Dowd, C. D.: Concentration and sources of atmospheric nitrous acid (HONO) at an urban site in Western China, Science of The Total Environment, 593-594, 165-172, https://doi.org/10.1016/j.scitotenv.2017.02.166, 2017.

Kleffmann, J., Gavriloaiei, T., Hofzumahaus, A., Holland, F., Koppmann, R., Rupp, L., Schlosser, E., Siese, M., and Wahner, A.: Daytime formation of nitrous acid: A major source of OH radicals in a forest, Geophysical Research Letters, 32, doi:10.1029/2005GL022524, 2005.

Kuang, Y., Zhao, C. S., Tao, J. C., and Ma, N.: Diurnal variations of aerosol optical properties in the North China Plain and their influences on the estimates of direct aerosol radiative forcing, Atmos. Chem. Phys. Discuss., 15, 339-369, 10.5194/acpd-15-339-2015, 2015.

Kuang, Y., Zhao, C., Tao, J., Bian, Y., Ma, N., and Zhao, G.: A novel method for deriving the aerosol hygroscopicity parameter based only on measurements from a humidified nephelometer system, Atmos. Chem. Phys., 17, 6651-6662, 10.5194/acp-17-6651-2017, 2017.

Kuang, Y., Zhao, C. S., Zhao, G., Tao, J. C., Xu, W., Ma, N., and Bian, Y. X.: A novel method for calculating ambient aerosol liquid water content based on measurements of a humidified nephelometer system, Atmospheric Measurement Techniques, 11, 2967-2982, 10.5194/amt-11-2967-2018, 2018.

Li, L., Duan, Z., Li, H., Zhu, C., Henkelman, G., Francisco, J. S., and Zeng, X. C.: Formation of HONO from the NH3-promoted hydrolysis of NO2-dimers in the atmosphere, Proceedings of the National Academy of Sciences, 10.1073/pnas.1807719115, 2018a.

Li, L., Hoffmann, M. R., and Colussi, A. J.: Role of Nitrogen Dioxide in the Production of Sulfate during Chinese Haze-Aerosol Episodes, Environmental science & technology, 10.1021/acs.est.7b05222, 2018b.

Li, X., Brauers, T., Häseler, R., Bohn, B., Fuchs, H., Hofzumahaus, A., Holland, F., Lou, S., Lu, K. D., Rohrer, F., Hu, M., Zeng, L. M., Zhang, Y. H., Garland, R. M., Su, H., Nowak, A., Wiedensohler, A., Takegawa, N., Shao, M., and Wahner, A.: Exploring the atmospheric chemistry of nitrous acid (HONO) at a rural site in Southern China, Atmospheric Chemistry and Physics, 12, 1497-1513, 10.5194/acp-12-1497-2012, 2012.

© Author(s) 2018. CC BY 4.0 License.

Liu, M., Song, Y., Zhou, T., Xu, Z., Yan, C., Zheng, M., Wu, Z., Hu, M., Wu, Y., and Zhu, T.: Fine particle pH during severe haze episodes in northern China, Geophysical Research Letters, 44, 5213-5221, doi:10.1002/2017GL073210, 2017a.

Liu, Y., Wu, Z., Wang, Y., Xiao, Y., Gu, F., Zheng, J., Tan, T., Shang, D., Wu, Y., Zeng, L., Hu, M., Bateman, A. P., and Martin, S. T.: Submicrometer Particles Are in the Liquid State during Heavy Haze Episodes in the Urban Atmosphere of Beijing, China, Environmental Science & Technology Letters, 4, 427-432, 10.1021/acs.estlett.7b00352, 2017b.

Liu, Z., Wang, Y., Costabile, F., Amoroso, A., Zhao, C., Huey, L. G., Stickel, R., Liao, J., and Zhu, T.: Evidence of Aerosols as a Media for Rapid Daytime HONO Production over China, Environmental science & technology, 48, 14386-14391, 10.1021/es504163z, 2014.

Lu, C., Niu, S., Tang, L., Lv, J., Zhao, L., and Zhu, B.: Chemical composition of fog water in Nanjing area of China and its related fog microphysics, Atmospheric Research, 97, 47-69, http://dx.doi.org/10.1016/j.atmosres.2010.03.007, 2010.

Lu, K., Guo, S., Tan, Z., Wang, H., Shang, D., Liu, Y., Li, X., Wu, Z., Hu, M., and Zhang, Y.: Exploring atmospheric free-radical chemistry in China: the self-cleansing capacity and the formation of secondary air pollution, National Science Review, nwy073-nwy073, 10.1093/nsr/nwy073, 2018.

Michoud, V., Colomb, A., Borbon, A., Miet, K., Beekmann, M., Camredon, M., Aumont, B., Perrier, S., Zapf, P., Siour, G., Ait-Helal, W., Afif, C., Kukui, A., Furger, M., Dupont, J. C., Haeffelin, M., and Doussin, J. F.: Study of the unknown HONO daytime source at a European suburban site during the MEGAPOLI summer and winter field campaigns, Atmos. Chem. Phys., 14, 2805-2822, 10.5194/acp-14-2805-2014, 2014.

Nie, W., Ding, A. J., Xie, Y. N., Xu, Z., Mao, H., Kerminen, V. M., Zheng, L. F., Qi, X. M., Huang, X., Yang, X. Q., Sun, J. N., Herrmann, E., Petäjä, T., Kulmala, M., and Fu, C. B.: Influence of biomass burning plumes on HONO chemistry in eastern China, Atmospheric Chemistry and Physics, 15, 1147-1159, 10.5194/acp-15-1147-2015, 2015.

Petters, M. D., and Kreidenweis, S. M.: A single parameter representation of hygroscopic growth and cloud condensation nucleus activity, Atmospheric Chemistry and Physics, 7, 1961-1971, 2007.

Ran, L., Zhao, C. S., Xu, W. Y., Lu, X. Q., Han, M., Lin, W. L., Yan, P., Xu, X. B., Deng, Z. Z., Ma, N., Liu, P. F., Yu, J., Liang, W. D., and Chen, L. L.: VOC reactivity and its effect on ozone production during the HaChi summer campaign, Atmos. Chem. Phys., 11, 4657-4667, 10.5194/acp-11-4657-2011, 2011.

Safai, P. D., Kewat, S., Pandithurai, G., Praveen, P. S., Ali, K., Tiwari, S., Rao, P. S. P., Budhawant, K. B., Saha, S. K., and Devara, P. C. S.: Aerosol characteristics during winter fog at Agra, North India, J. Atmos. Chem., 61, 101-118, 10.1007/s10874-009-9127-4, 2008.

Song, S., Gao, M., Xu, W., Shao, J., Shi, G., Wang, S., Wang, Y., Sun, Y., and McElroy, M. B.: Fine-particle pH for Beijing winter haze as inferred from different thermodynamic equilibrium models, Atmos. Chem. Phys., 18, 7423-7438, 10.5194/acp-18-7423-2018, 2018.

Su, H., Cheng, Y., Oswald, R., Behrendt, T., Trebs, I., Meixner, F. X., Andreae, M. O., Cheng, P., Zhang, Y., and Pöschl, U.: Soil Nitrite as a Source of Atmospheric HONO and OH Radicals, Science, 333, 1616-1618, 10.1126/science.1207687, 2011.

Wang, G., Zhang, R., Gomez, M. E., Yang, L., Levy Zamora, M., Hu, M., Lin, Y., Peng, J., Guo, S., Meng, J., Li, J., Cheng, C., Hu, T., Ren, Y., Wang, Y., Gao, J., Cao, J., An, Z., Zhou, W., Li, G., Wang, J., Tian, P., Marrero-Ortiz, W., Secrest, J., Du, Z., Zheng, J., Shang, D., Zeng, L., Shao, M., Wang, W., Huang, Y., Wang, Y., Zhu, Y., Li, Y., Hu, J., Pan, B., Cai, L., Cheng, Y.,

© Author(s) 2018. CC BY 4.0 License.

Ji, Y., Zhang, F., Rosenfeld, D., Liss, P. S., Duce, R. A., Kolb, C. E., and Molina, M. J.: Persistent sulfate formation from London Fog to Chinese haze, Proceedings of the National Academy of Sciences, 113, 13630, 2016a.

Wang, G., Zhang, R., Gomez, M. E., Yang, L., Levy Zamora, M., Hu, M., Lin, Y., Peng, J., Guo, S., Meng, J., Li, J., Cheng, C., Hu, T., Ren, Y., Wang, Y., Gao, J., Cao, J., An, Z., Zhou, W., Li, G., Wang, J., Tian, P., Marrero-Ortiz, W., Secrest, J., Du, Z., Zheng, J., Shang, D., Zeng, L., Shao, M., Wang, W., Huang, Y., Wang, Y., Zhu, Y., Li, Y., Hu, J., Pan, B., Cai, L., Cheng, Y., Ji, Y., Zhang, F., Rosenfeld, D., Liss, P. S., Duce, R. A., Kolb, C. E., and Molina, M. J.: Persistent sulfate formation from London Fog to Chinese haze, Proc Natl Acad Sci U S A, 10.1073/pnas.1616540113, 2016b.

Wu, Z., Wang, Y., Tan, T., Zhu, Y., Li, M., Shang, D., Wang, H., Lu, K., Guo, S., Zeng, L., and Zhang, Y.: Aerosol Liquid Water Driven by Anthropogenic Inorganic Salts: Implying Its Key Role in Haze Formation over the North China Plain, Environmental Science & Technology Letters, 10.1021/acs.estlett.8b00021, 2018.

Xing, J., Ding, D., Wang, S., Zhao, B., Jang, C., Wu, W., Zhang, F., Zhu, Y., and Hao, J.: Quantification of the enhanced effectiveness of NOx control from simultaneous reductions of VOC and NH3 for reducing air pollution in the Beijing–Tianjin–Hebei region, China, Atmos. Chem. Phys., 18, 7799-7814, 10.5194/acp-18-7799-2018, 2018.

Xu, W. Y., Zhao, C. S., Ran, L., Lin, W. L., Yan, P., and Xu, X. B.: SO2 noontime-peak phenomenon in the North China Plain, Atmospheric Chemistry and Physics, 14, 7757-7768, 10.5194/acp-14-7757-2014, 2014.

Yabushita, A., Enami, S., Sakamoto, Y., Kawasaki, M., Hoffmann, M. R., and Colussi, A. J.: Anion-Catalyzed Dissolution of NO2 on Aqueous Microdroplets, The Journal of Physical Chemistry A, 113, 4844-4848, 10.1021/jp900685f, 2009.

Yin, Z., Ye, X., Jiang, S., Tao, Y., Shi, Y., Yang, X., and Chen, J.: Size-resolved effective density of urban aerosols in Shanghai, Atmospheric Environment, 100, 133-140, http://dx.doi.org/10.1016/j.atmosenv.2014.10.055, 2015.

Young, L.-H., Li, C.-H., Lin, M.-Y., Hwang, B.-F., Hsu, H.-T., Chen, Y.-C., Jung, C.-R., Chen, K.-C., Cheng, D.-H., Wang, V.-S., Chiang, H.-C., and Tsai, P.-J.: Field performance of a semi-continuous monitor for ambient PM2.5 water-soluble inorganic ions and gases at a suburban site, Atmospheric Environment, 144, 376-388, https://doi.org/10.1016/j.atmosenv.2016.08.062, 2016.

Zheng, G. J., Duan, F. K., Su, H., Ma, Y. L., Cheng, Y., Zheng, B., Zhang, Q., Huang, T., Kimoto, T., Chang, D., Pöschl, U., Cheng, Y. F., and He, K. B.: Exploring the severe winter haze in Beijing: the impact of synoptic weather, regional transport and heterogeneous reactions, Atmos. Chem. Phys., 15, 2969-2983, 10.5194/acp-15-2969-2015, 2015.

Atmos. Chem. Phys. Discuss., https://doi.org/10.5194/acp-2018-996
Manuscript under review for journal Atmos. Chem. Phys.
Discussion started: 30 November 2018
© Author(s) 2018. CC BY 4.0 License.

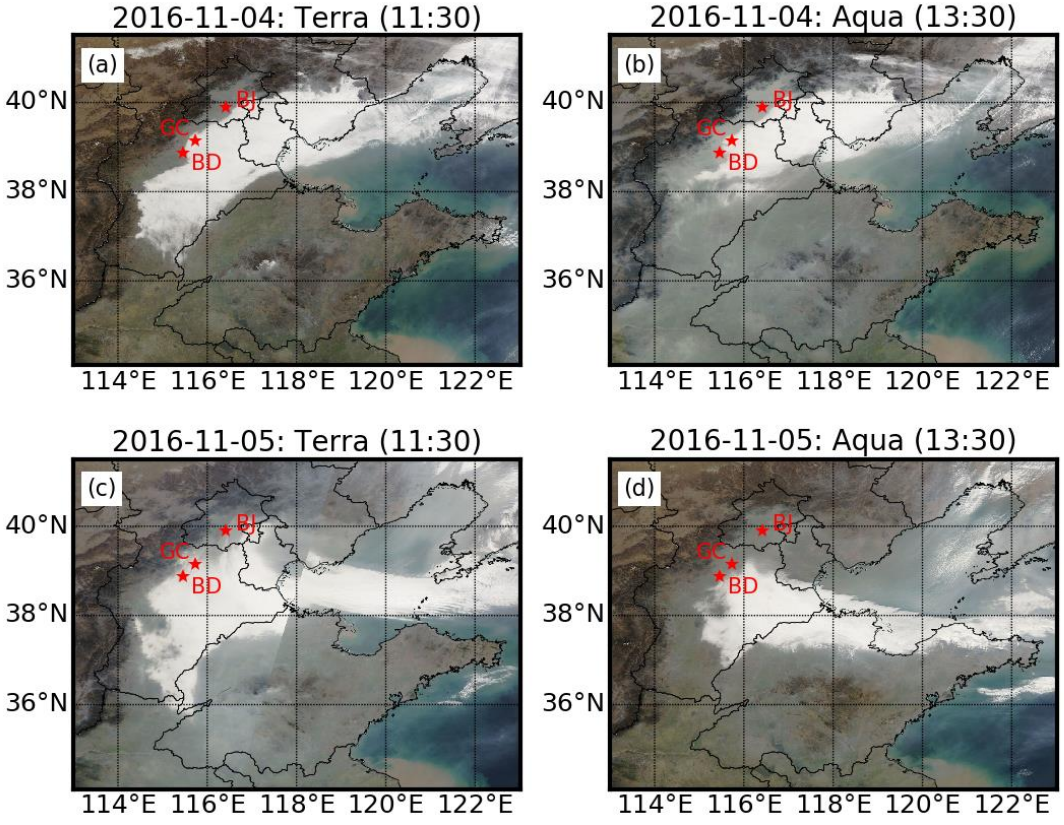

Figure 1. MODIS Terra (a,c) and Aqua (b,d) satellite images in 2016-11-04 (a,b) and 2016-11-05 (c,d), star markers are locations of Gucheng (GC: the observation site), Baoding (BD) and Beijing (BJ).

Atmos. Chem. Phys. Discuss., https://doi.org/10.5194/acp-2018-996
Manuscript under review for journal Atmos. Chem. Phys.
Discussion started: 30 November 2018
© Author(s) 2018. CC BY 4.0 License.

Atmospheric Chemistry and Physics Discussions

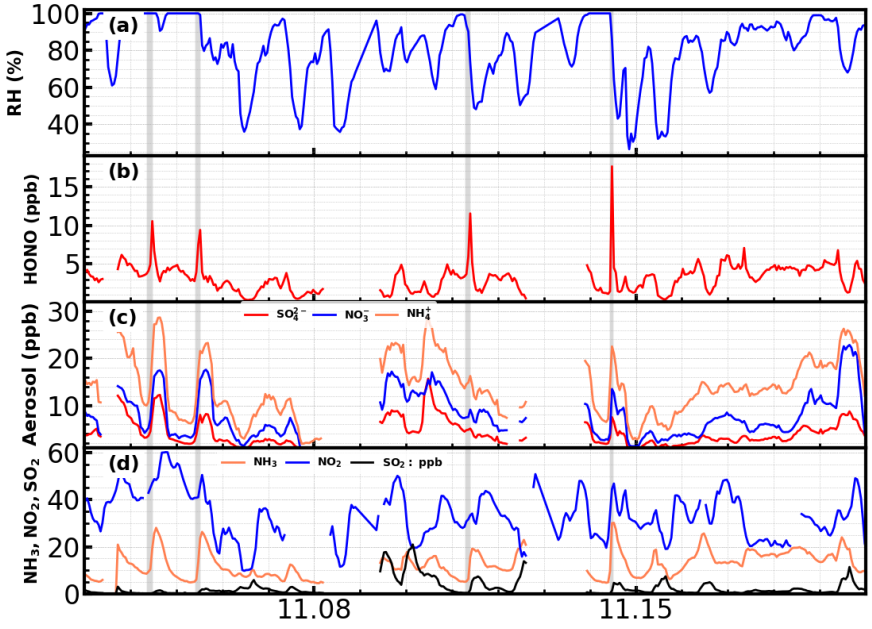

538

539 **Figure 2**. Time series of ambient **a)** RH; **b)** HONO; **c)** sulfate, nitrate, ammonium; **d)** NH_3, NO_3
540 and SO_2 during the observation period.
541

Atmos. Chem. Phys. Discuss., https://doi.org/10.5194/acp-2018-996
Manuscript under review for journal Atmos. Chem. Phys.
Discussion started: 30 November 2018
© Author(s) 2018. CC BY 4.0 License.

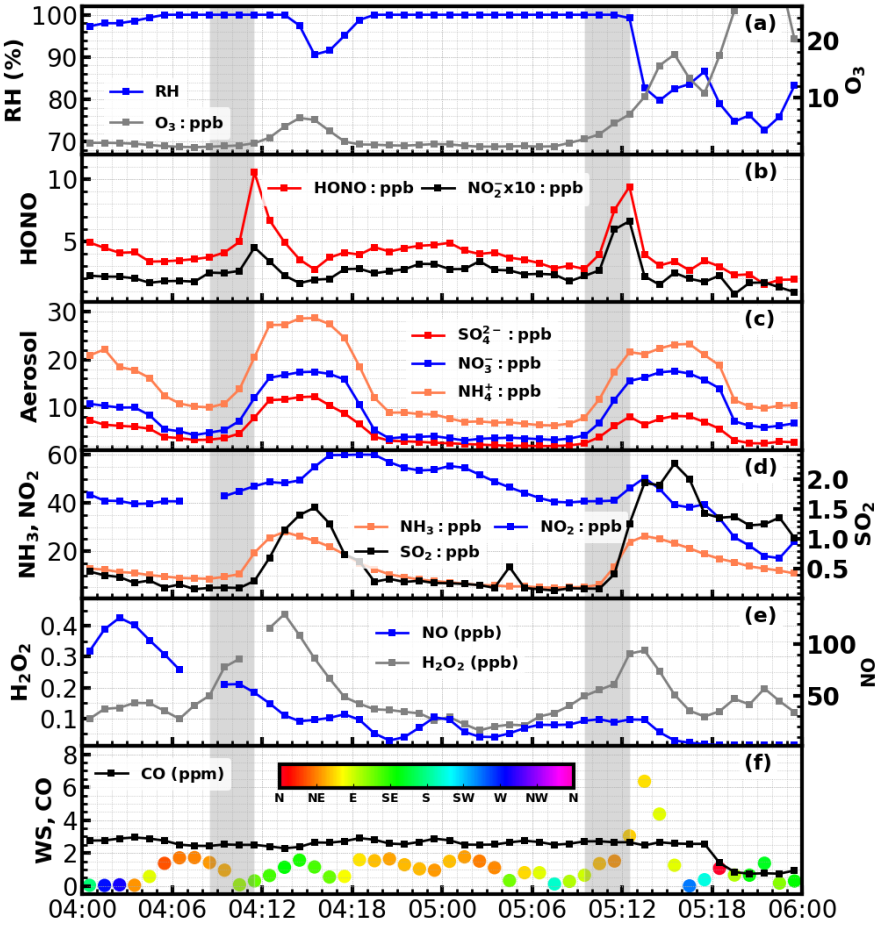

Figure 3. Time series of ambient **a)** RH,O_3, **b)**HONO, NO_2^-, **c)** SO_4^{2-}, NO_3^-, NH_4^+, **d)** NH_3, NO_2, SO_2, **e)** NO, H_2O_2, **f)** CO, wind speed and wind direction (colors of scatter points) from 11-04 to 11-05. Gray shaded areas represent periods of rapid increase of HONO.

Atmos. Chem. Phys. Discuss., https://doi.org/10.5194/acp-2018-996
Manuscript under review for journal Atmos. Chem. Phys.
Discussion started: 30 November 2018
© Author(s) 2018. CC BY 4.0 License.

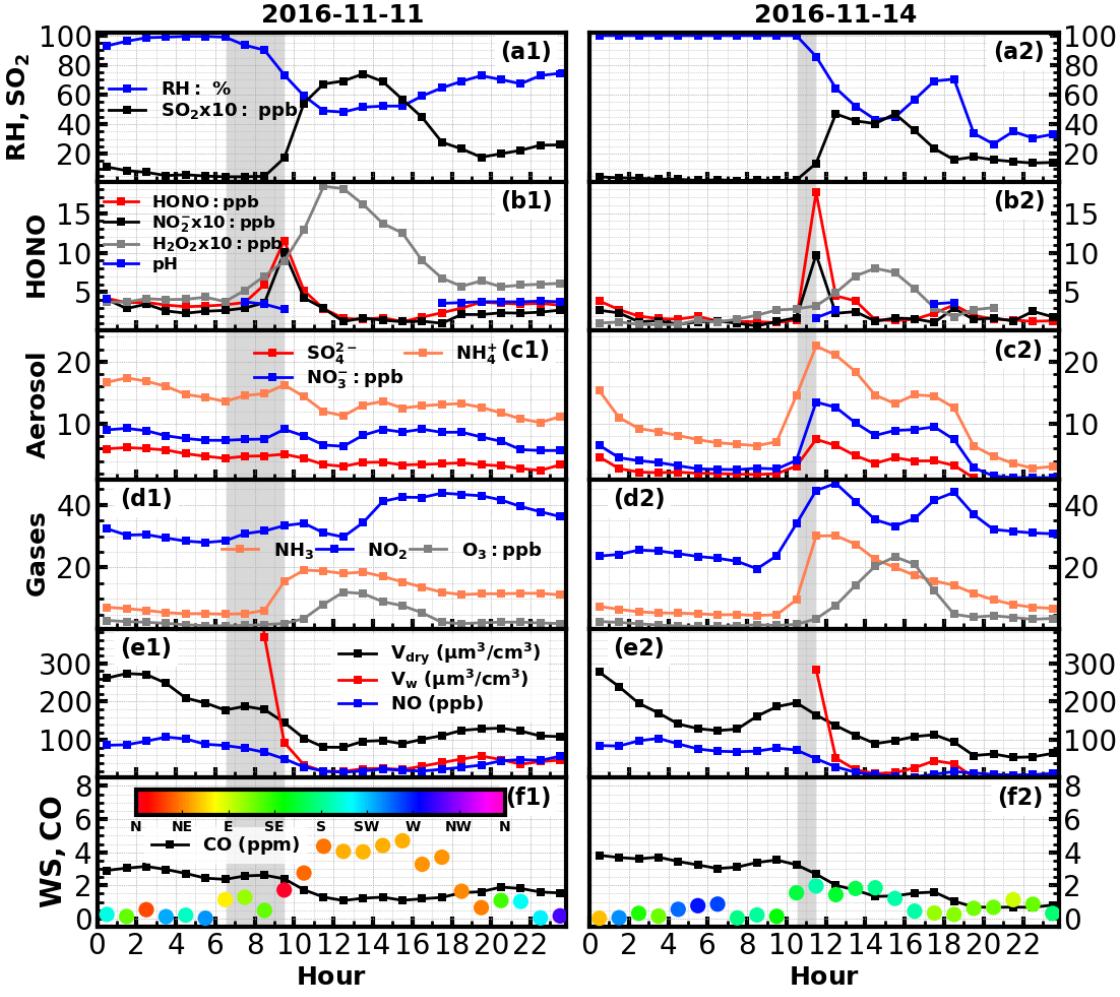

Figure 4. Time series of ambient **a)** RH, SO_2, **b)** HONO, NO_2^-, H_2O_2, aerosol pH, **c)** SO_4^{2-}, NO_3^-, NH_4^+,**d)** NH_3, NO_2, O_3, **e)** NO, volume concentrations of $PM_{2.5}$ in dry state (V_{dry}), volume concentrations of liquid water (V_w), **f)** CO, wind speed and wind direction during **1)** 11th Nov. 2016 and **2)** 14th Nov. 2016. Gray shaded areas represents periods of rapid increase of HONO.

Atmos. Chem. Phys. Discuss., https://doi.org/10.5194/acp-2018-996
Manuscript under review for journal Atmos. Chem. Phys.
Discussion started: 30 November 2018
© Author(s) 2018. CC BY 4.0 License.

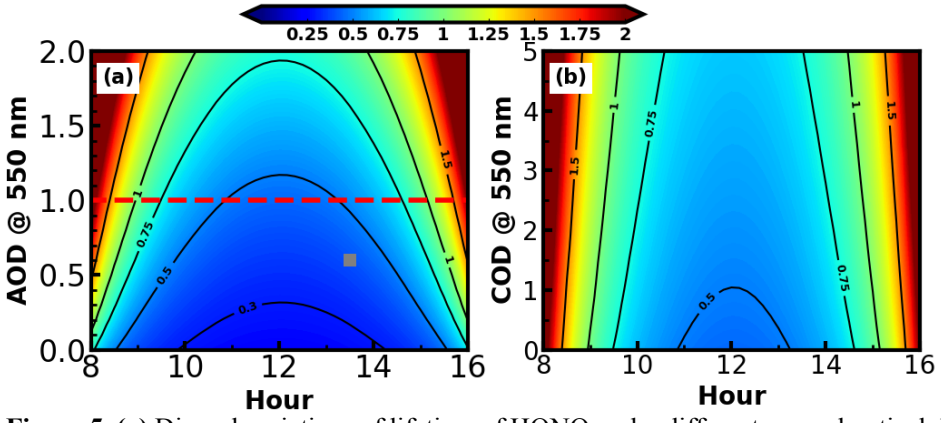

Figure 5. **(a)** Diurnal variations of lifetime of HONO under different aerosol optical depth (AOD) conditions. Gray solid marker represents the AOD position from MODIS Aqua in 2016-11-14 (about 13:30); **(b)** Diurnal variations of lifetime of HONO under different cloud optical depth (COD) conditions, with an AOD of 1.

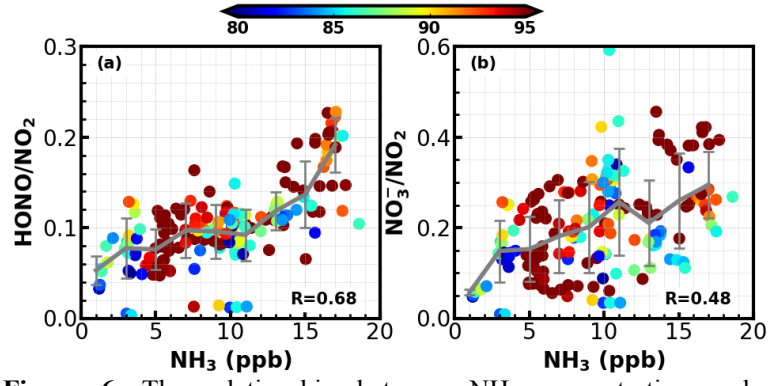

Figure 6. The relationship between NH_3 concentration and **a)** $HONO/NO_2$ ratio; **b)** nitrate/nitrogen dioxide ratio (NO_3^-/NO_2); Colors of scatter points represent ambient RHs and the color bar is shown on the top.

Atmos. Chem. Phys. Discuss., https://doi.org/10.5194/acp-2018-996
Manuscript under review for journal Atmos. Chem. Phys.
Discussion started: 30 November 2018
© Author(s) 2018. CC BY 4.0 License.

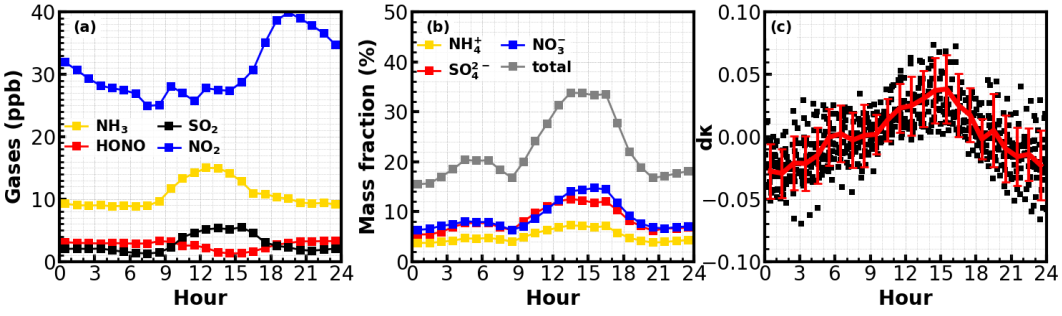

Figure 7. **(a)** Average diurnal variations of Gases ; **(b)** Average diurnal variations mass fractions of nitrate, sulfate and ammonium; **(c)** Diurnal variations of aerosol hygroscopicity, dκ is the anomaly to the daily mean κ.